PLOTS OF THE SPIN-LATTICE RELAXATION TIME AND NUCLEAR OVERHAUSER ENHANCEMENT NMR VALUES YIELDING A SPREAD DISTRIBUTION OF THE ROTATIONAL CORRELATION TIME

Jaromír JAKEŠ

Institute of Macromolecular Chemistry, Academy of Sciences of the Czech Republic, Heyrovského nám. 2, 162 06 Prague 6, Czech Republic; e-mail: jakes@imc.cas.cz

Received November 26, 1999
Accepted January 20, 2000

It is shown, that the plots of ω/T_1 and NOE × ω/T_1 *versus* –log ω give the distribution of rotational correlation time τ plotted *versus* log τ and spread by (rather wide) "slit" functions the form and shape of which are independent of the position on the log τ axis. When plotting data at various temperatures, temperature shift factors a_T and the plots *versus* –log (ωa_T) should be used. The plots permit to check the data compatibility and are helpful in studying molecular dynamics. Examples of the plots are given. One example stimulated a consideration of the segmental motion dynamics, which showed that the Hall–Helfand distribution is inappropriate for a description of the orientational relaxation of the non-backbone (C–H) bonds in a polymer chain.

Key words: NMR spectroscopy; Nuclear magnetic resonance; Spin-lattice relaxation; Nuclear Overhauser enhancement; Graphical correlation; Polymer chain segmental motions; Rotational autocorrelation function; Molecular dynamics.

Studying molecular dynamics by NMR is based on the fact that nuclear magnetic spin relaxation is effected by molecular motions[1]. Dipole–dipole interactions, spin-rotation, chemical shift anisotropy, and quadrupolar interaction are mechanisms influencing the spin-lattice relaxation time T_1. In ^{13}C nuclei with directly bonded protons, the first mechanism is predominant, whereas in quadrupolar nuclei the last one prevails; contributions of other mechanisms may often be neglected. Considering purely ^{13}C-^{1}H dipolar mechanism in ^{13}C nuclei, we obtain[2]

$$\frac{1}{T_1} = \frac{N}{10}\left(\hbar\gamma_H\gamma_C / r_{CH}^3\right)^2 \left(J(\omega_H - \omega_C) + 3J(\omega_C) + 6J(\omega_H + \omega_C)\right), \qquad (1)$$

where N is the number of protons directly bonded at the distance r_{CH} to the ^{13}C nucleus, $\hbar = h/(2\pi)$ is the reduced Planck constant, γ_H and γ_C are the

magnetogyric ratios of the respective nuclei, ω_H and ω_C are the resonance (Larmor) frequencies of the respective nuclei, and $J(\omega)$ is the Fourier transform of the normalized second-order spherical harmonic autocorrelation function $G(t)$,

$$G(t) = \frac{3}{2}\left\langle \cos^2 \theta(t) \right\rangle - \frac{1}{2}\,, \tag{2}$$

where $\theta(t)$ is the angle between the direction of the ^{13}C–H bond at the time 0 and that at the time t. For the case of an isotropic rotational reorientation,

$$G(t) = \exp\left(-t / \tau_R\right) \tag{3}$$

and

$$J(\omega) = \tau_R / \left(1 + \omega^2 \tau_R^2\right), \tag{4}$$

where τ_R is the rotational correlation time. For purely quadrupolar relaxation of deuterium nuclei, Eq. (*5*) holds[3]

$$\frac{1}{T_1} = \frac{3}{10}\pi^2 \chi^2 \left(J(\omega_D) + 4J(2\omega_D)\right), \tag{5}$$

where χ is the deuterium quadrupolar coupling constant and other symbols have the same meaning as in Eq. (*1*). Nuclear Overhauser enhancement[4] (NOE) is another source of information about the molecular motion. Under conditions of validity of Eq. (*1*), NOE is given by[5]

$$\mathrm{NOE} = 1 + \frac{\gamma_H}{\gamma_C} \frac{6J(\omega_H + \omega_C) - J(\omega_H - \omega_C)}{J(\omega_H - \omega_C) + 3J(\omega_C) + 6J(\omega_H + \omega_C)}\,. \tag{6}$$

When the molecular motion is more complicated than an isotropic rotational reorientation, Eqs (3) and (*4*) no longer hold. For the jump-like or diffusive motions, they should be replaced by

$$G(t) = \sum_{i=1}^{r} w_i \exp(-t / \tau_i) \tag{7}$$

and

$$J(\omega) = \sum_{i=1}^{r} w_i \tau_i / \left(1 + \omega^2 \tau_i^2\right) \tag{8}$$

with amplitudes $w_i > 0$ and $\sum_{i=1}^{r} w_i = 1$. In the jump-like case, $1/\tau_i$ values are some of the eigenvalues λ_i of a matrix compiled from the jump rates (jump probabilities) and, in the diffusive case, some of the eigenvalues of the differential equation obtained by separating off the time variable from the diffusive equation. In the latter case, r may be infinite. For the free diffusive rotation, with the correlation time τ_G, of a bond around an axis inclined by an angle θ from the bond, $\lambda_i = (i - 1)^2/(6\tau_G)$, $i = 1, 2, 3, 4, \ldots$, however, only the first three $1/\lambda_i = \tau_i$ may appear with non-zero w_i in Eqs (*7*) and (*8*). When, in addition, the molecule undergoes an isotropic reorientation of the correlation time τ_R, $r = 3$, $\tau_1 = \tau_R$, $w_1 = (\frac{3}{2}\cos^2\theta - \frac{1}{2})^2$, $1/\tau_2 = 1/\tau_R + 1/(6\tau_G)$, $w_2 = 3\sin^2\theta\cos^2\theta$, $1/\tau_3 = 1/\tau_R + 4/(6\tau_G)$, and $w_3 = \frac{3}{4}\sin^4\theta$ hold[5] in Eqs (*7*) and (*8*). When the system is infinite, the correlation time τ distribution becomes continuous and Eq. (*8*) should be rewritten as

$$J(\omega) = \int_0^\infty w(\tau)\,\tau\left(1 + \omega^2\tau^2\right)^{-1} \mathrm{d}\tau \tag{9}$$

with $w(\tau) \geq 0$ and $\int_0^\infty w(\tau)\,\mathrm{d}(\tau) = 1$. Introducing $w(\tau)$ in the form of a sum of δ-functions, Eq. (*9*) is brought back to Eq. (*8*).

Considering dynamics of a polymer chain in the random coil state is a rather difficult problem. Hence, Schaefer[6] used an empirical log χ^2 distribution for $w(\tau)$. This distribution is based on the χ^2 distribution (called also Schulz–Zimm distribution) applied to the variable $\log(1 + (b - 1)\tau/\bar{\tau})/\log b$ with $\bar{\tau}$ being the average correlation time and with b usually set to 1 000. Another empirical distribution of the correlation time (in studying mechanical properties, called relaxation time), the power-law one of the form

$$w(\tau) = |p|\,\tau^{p-1}\tau_0^{-p} \ , \tag{10}$$

spreading from zero to τ_0 for positive and from τ_0 to infinity for negative p, is frequently used in studying viscoelastic properties of macromolecules.

In polymer chain dynamics studies, the chain atoms are often assumed to be located in the diamond lattice[7] sites. In the condensed phase, the free volume necessary for allowing a motion is usually decisive for the motion rate. The three-bond motion[7] needs the least free volume, the four-bond motion[7] needs little more. The former leaves the direction of the central moving bond unchanged and exchanges the directions of the terminal moving bonds, in fact effecting a diffusion of bond directions among odd and among even bonds along the chain. On this basis, Hall and Helfand[8] considered a chain, in which correlated exchanges of bond directions among neighbouring elements appeared at the rate λ_1 and uncorrelated changes of bond directions at the rate λ_0, obtaining

$$w(\tau) = \pi^{-1}\tau^{-1}\left((1-\tau/\tau_0)(\tau/\tau_1 - 1)\right)^{-1/2} \qquad (11)$$

for $\tau_1 < \tau < \tau_0$ and $w(\tau) = 0$ elsewhere; $1/\tau_0 = 2\lambda_0$ and $1/\tau_1 = 2\lambda_0 + 4\lambda_1$. The distribution defined by Eq. (*11*), extending from τ_1 to τ_0, will be hereinafter called the Hall–Helfand (HH) distribution and denoted by $H(\tau; \tau_0, \tau_1)$. Then

$$J(\omega) = \mathrm{Re}\left[\left(1/\tau_0 - \mathrm{i}\omega\right)^{-1/2}\left(1/\tau_1 - \mathrm{i}\omega\right)^{-1/2}\right], \qquad (12)$$

where Re means the real part and i means the imaginary unit. Such an approach neglects the backstep effect, *i.e.*, the fact that the two neighbours of a chain atom cannot occupy the same lattice location after the three-bond jump, which hinders the diffusion of bond directions along the chain. The backstep effect was considered by Dubois–Violette *et al.*[9] (DV), yielding a distortion of the distribution given by Eq. (*11*) with $\tau_0 = \infty$.

In a simulation of the chain motion, Geny and Monnerie[10] confirmed the $t^{-1/2}$ decay of $G(t)$ at long delay time t, found by DV. In another simulation, Weber and Helfand[11] considered molecular dynamics of a polyethylene chain and calculated $G(t)$ for some unit vectors in the chain. The $G(t)$'s of the vector bisecting the C–C–C angle and the out-of-plane vector could well be fitted by Eq. (*11*) with finite τ_0, whereas those of the C–C bond vector and of the vector joining next-but-one C neighbours required an addition of a long correlation time $\tau_2 > \tau_0$ in the form

$$w(\tau) = (1-\alpha)H(\tau; \tau_0, \tau_1) + \alpha\delta(\tau - \tau_2) . \qquad (13)$$

The appearance of τ_2 was assigned[11] to a slow relaxation of the end-to-end distance of the molecular chain.

Dejean, Lauprêtre, and Monnerie[12] (DLM) considered, in addition to the Hall–Helfand model[8], a fast anisotropic libration of the ^{13}C–H bond with the correlation time $\tau_2 << \tau_1$ and reached

$$w(\tau) = (1-\alpha)H(\tau; \tau_0, \tau_1) + \alpha H(\tau; \tau_0\tau_2/(\tau_0 + \tau_2), \tau_1\tau_2/(\tau_1 + \tau_2)) . \qquad (14)$$

(Note that τ_0 and τ_2 are interchanged in ref.[12] and $1/\tau_1$ in this paper equals $1/\tau_2 + 2/\tau_1$ there.) Replacing $H(\tau; \tau_0\tau_2/(\tau_0 + \tau_2), \tau_1\tau_2/(\tau_1 + \tau_2))$ by $\delta(\tau - \tau_2)$ (which is a good approximation for $\tau_2 << \tau_1$), they again obtained Eq. (*13*), but with $\tau_2 << \tau_1$. Equation (*13*) with such τ_2 succeeded in good fitting backbone ^{13}C T_1 values of poly(methyl vinyl ether)[12] and ^{13}C T_1 and NOE values of poly(vinyl chloride)[13], all measured at two resonance frequencies ω_C and several temperatures. At that, in changing temperature, $\tau w(\tau)$ was always assumed just shifted on log τ scale without any shape change.

Usually, T_1 and NOE data are too scarce for studying the correlation time τ distribution: data at two[12–14] or three[3,15,16] resonance frequencies are usual; more data (at five[17] or seven[18] frequencies) are rather an exception. A way to overcome this difficulty is to correlate data at various temperatures. Such an approach is commonly used with viscoelastic data[19]. It was found that assuming the same temperature dependence (the same ratio at different temperatures) for all correlation times and the temperature independence of the amplitudes was often a good approximation in considering dynamic moduli data G' and G''. Then

$$w_T(\tau) = w_{T_0}(\tau / a_T) / a_T , \qquad (15)$$

where $w_T(\tau)$ is the correlation time distribution at temperature T, a_T is the temperature shift factor, and T_0 is the reference temperature; $a_{T_0} = 1$. This means that in changing temperature from T_0 to T, the $\tau w(\tau)$ distribution function plotted *versus* log τ is just shifted by log a_T on the log τ axis without any shape change. Note that in shifting a discrete τ distribution (Eqs (*7*) and (*8*)), the w_i amplitudes are left unchanged (are not divided by a_T).

Equation (*15*) was used in interpreting T_1 and NOE data[12,13], although its use was not explicitly stated. On the other hand, a narrowing of the τ distribution with increasing temperature was found[3] when log χ^2 distribution[6] of τ was used.

The temperature dependence of a_T should be smooth. Expressing the temperature dependence of the decorrelation rate, 1/τ, by the Arrhenius equation yields

$$a_T = \exp\left(\frac{\Delta H}{\boldsymbol{R}}\left(\frac{1}{T} - \frac{1}{T_0}\right)\right). \qquad (16)$$

Equation (*16*) often works well in dilute polymer solutions and in bulk polymers well above the glass transition temperature. With a correction for the temperature dependence of the solvent viscosity, it was successfully used[16] in interpreting T_1 and NOE data of polyisoprene dissolved in toluene-d_8. Slightly above the glass transition temperature, Eq. (*16*) should be replaced by[20]

$$a_T = \exp\left(A/\left(T - T_\infty\right) - A/\left(T_0 - T_\infty\right)\right), \qquad (17)$$

where A and T_∞ are adjustable parameters. This is due to the dominant role of the free volume temperature change in the temperature change of the correlation time distribution in this temperature region[19].

The object of this paper is to suggest plots of the T_1 and NOE NMR values measured at various resonance frequencies and various temperatures, giving a spread distribution of the correlation time τ, and to show examples of such plots. A consideration of the segmental motion dynamics stimulated at examining one of the plots is also presented.

THEORY

Introducing Eq. (*9*) into Eq. (*1*), (*6*), or (*5*), multiplying by ω_C or ω_D, and normalizing properly, we obtain

$$f_i(\omega_i) = \int_0^\infty w(\tau)\, K_i(\omega_i \tau)\, \mathrm{d}\tau\,, \qquad (18)$$

where the subscript i = 1, 2, or 3 refers to Eq. (*1*), (*6*), or (*5*), respectively, $\omega_1 = \omega_2 = \omega_C$, $\omega_3 = \omega_D$, $f_1(\omega_C) = 20\, r_{CH}^6 \ln 10 \times \omega_C/([6/(R+1) + 3 + 1/(R-1)]\pi N(\hbar\gamma_H\gamma_C)^2 T_1)$, $K_1(x) = [6L((R+1)x)/(R+1) + 3L(x) + L((R-1)x)/(R-1)] \times 2 \ln 10/([6/(R+1) + 3 + 1/(R-1)]\pi)$, $f_2(\omega_C) = 5\, r_{CH}^6 \ln 10 \times \mathrm{NOE} \times \omega_C/(2\pi N(\hbar\gamma_H\gamma_C)^2 T_1)$, $K_2(x) = [6L((R+1)x) + 3L(x) - L((R-1)x)] \times \ln 10/(4\pi)$, $f_3(\omega_D) = 20 \ln 10 \times \omega_D/(9\pi^3\chi^2 T_1)$, and $K_3(x) = (L(x) + 2L(2x)) \times 2 \ln 10/(3\pi)$; $R = \gamma_H/\gamma_C$ and $L(z) = z/(1+z^2)$. Normalization is chosen so as to yield $\int_{-\infty}^{\infty} K_i(x)\, \mathrm{d} \log x = 1$, then also $\int_{-\infty}^{\infty} f_i(\omega_i)\, \mathrm{d} \log \omega_i = 1$ in view of $\int_0^{\infty} w(\tau)\, \mathrm{d}\tau = 1$. Since the kernel $K_i(\omega_i, \tau)$ is a function of just the product $\omega_i\tau$, using a logarithmic scale, we have a convolution plus a reversal of the logarithmic axis. This means, plotting ω_C/T_1 *versus* –log ω_C, NOE × ω_C/T_1 *versus* –log ω_C, or ω_D/T_1 *versus* –log ω_D, each properly scaled, we obtain a plot of $\tau w(\tau)$ function *versus* log τ spread by a (rather wide) "slit" function, whose form and width are independent of the position on the log τ axis. The "slit" functions (showing the spread plots for $w(\tau) = \delta(\tau - 1)$) are shown in Fig. 1.

Introducing Eq. (*15*) into Eq. (*18*), we can see that

$$f_{i,T}(\omega_i) = f_{i,T_0}(a_T \omega_i)\,. \qquad (19)$$

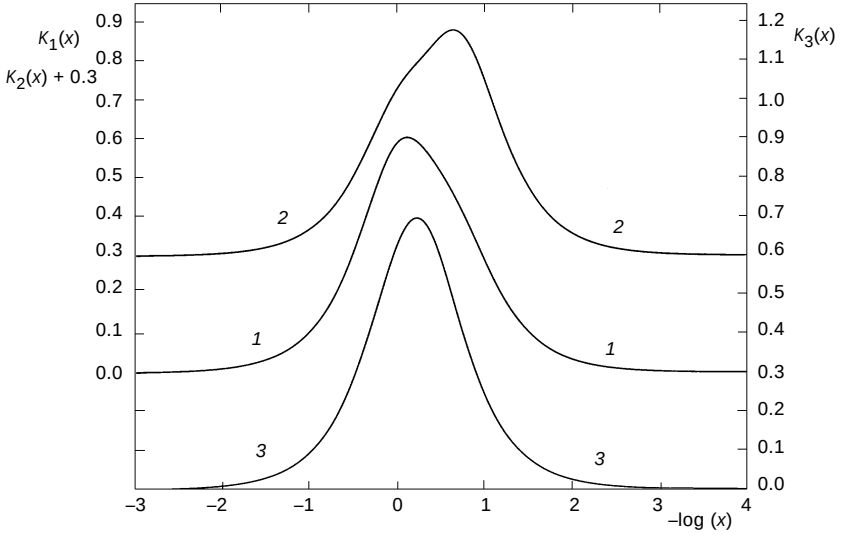

FIG. 1

"Slit" functions $K_i(x)$ (Eq. (*18*)) plotted *versus* –log (*x*). The scaled plots: *1* ω_C/T_1 *versus* –log ω_C (i = 1), *2* NOE × ω_C/T_1 *versus* –log ω_C (i = 2), *3* ω_D/T_1 *versus* –log ω_D (i = 3) show the spread rotational correlation time τ distribution function $\tau w(\tau)$ plotted *versus* log τ as viewed through these "slit" functions

Hence, plotting $f_{i,T}(\omega_i)$ values at various temperatures *versus* –log $(a_T\omega_i)$, we should obtain a single smooth curve, which is the spread $\tau w_{T_0}(\tau)$ distribution plotted *versus* log τ. A similar plot of the T_1 values was presented[15] using (somewhat ambiguous) characteristic frequencies at various temperatures in place of the shift factors a_T and not recognizing that the plot represents a spread τ distribution. With scarce NMR data, it is impossible to pick up the shift factors a_T by graphically superimposing $f_i(\omega)$ functions at various temperatures as is usual with viscoelastic data. Instead, a_T factors should be refined simultaneously with the parameters of the chosen $w(\tau)$ function using least squares. Also, it is impossible to check the validity of approximating the temperature dependence of the correlation time distribution with Eq. (*15*) by seeing whether superimposed $f_i(\omega)$ functions match in overlaps; this approximation should be introduced *ad hoc* relying on the fact that it mostly works with viscoelastic data. An invalidity of Eq. (*15*) may be traced when Eq. (*15*) fails to give a good data fit and much better data fits can be obtained for individual temperatures with a reasonable temperature dependence of parameters of $w(\tau)$.

It is desirable to have a graphic correlation of NMR relaxation data at various temperatures to consider the data compatibility before a calculation of parameters of the $w(\tau)$ function is started. For the above plot (Eq. (*19*)), a trial temperature dependence of the shift factors a_T should then be used. Using Eq. (*16*) with a few trial $\Delta H/\boldsymbol{R}$ values seems best. As an example, $f_1(\omega_C)$ and $f_2(\omega_C)$ values (scaled ω_C/T_1 and NOE × ω_C/T_1) measured[13] at various temperatures and two resonance frequencies for methylene ^{13}C nucleus in poly(vinyl chloride) dissolved in 1,1,2,2-tetrachloroethane-d_2 are plotted *versus* –log $(a_T\omega_C)$ in Fig. 2 using Eq. (*16*) with three different $\Delta H/\boldsymbol{R}$ values. We can see the temperature dependences of $f_i(\omega_C)$ at the two resonance frequencies. Their mutual position shows that the $\Delta H/\boldsymbol{R}$ value of 2 000 K is too small, that of 4 000 K is too large, and that of 3 000 K (*i.e.*, ΔH of 24.941 kJ/mol or 5.959 kcal/mol) is roughly correct. (Note that a least-squares adjustment using Eq. (*8*) with $r = 4$ yields $\Delta H/\boldsymbol{R}$ of 3 310 K.) Alternatively, the a_T factors may be picked out by the graphic method[15], developed for obtaining the temperature dependence of characteristic frequencies.

EXAMPLES AND DISCUSSION

As the first example, the plot of experimental $f_1(\omega_C)$ values (*i.e.*, scaled ω_C/T_1) measured at a single temperature *versus* –log ω_C is shown in Fig. 3 together with $f_1(\omega_C)$ calculated according to Eq. (*8*) with $r = 2$ and with w_i and τ_i adjusted by least squares. The 1.325 μs correlation time τ may be assigned

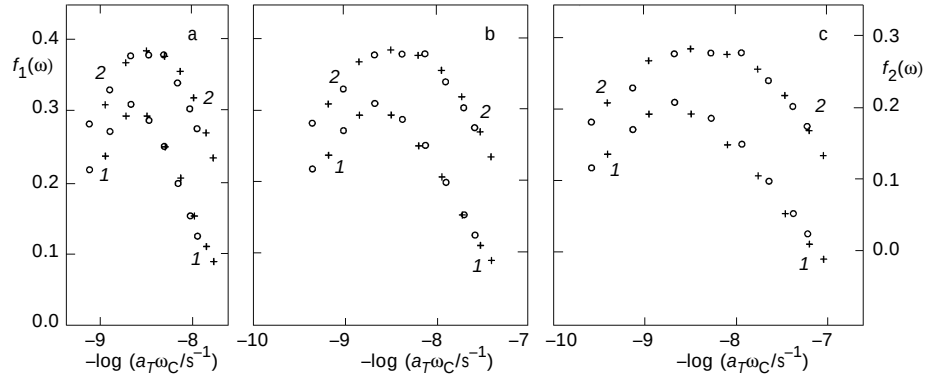

FIG. 2

Plots *versus* –log ($a_T\omega_C$) of $f_1(\omega_C)$ (*i.e.*, scaled ω_C/T_1 (*1*)) and $f_2(\omega_C)$ (*i.e.*, scaled NOE × ω_C/T_1 (*2*)) values measured[13] for methylene ^{13}C nucleus in poly(vinyl chloride) dissolved in 1,1,2,2-tetrachloroethane-d_2. a_T = exp ($\Delta H/(\boldsymbol{R}T) - \Delta H/(\boldsymbol{R}T_0)$), T_0 = 20 °C. The resonance frequency: + 50.3 MHz, ❍ 75.4 MHz. The values of $\Delta H/\boldsymbol{R}$: a 2 000 K, b 3 000 K, c 4 000 K

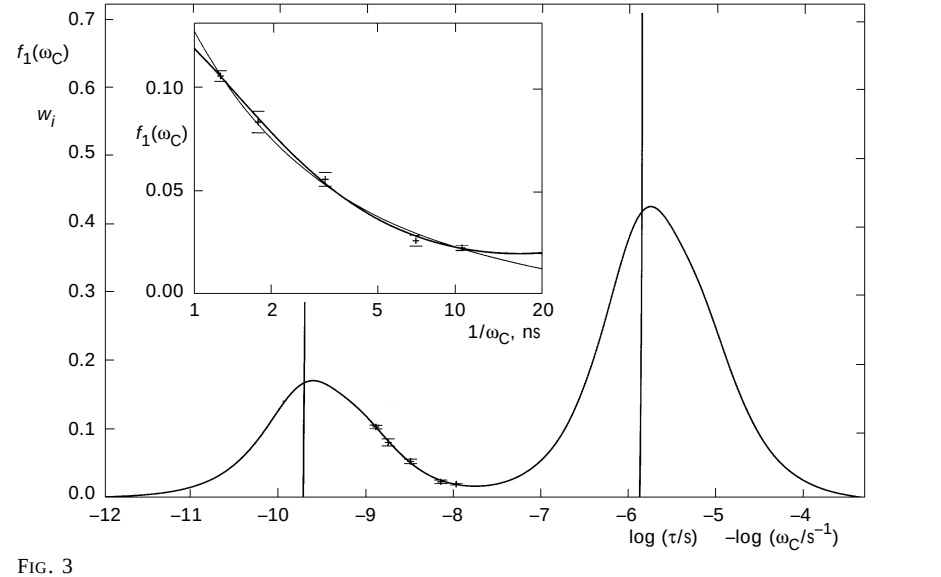

FIG. 3

A plot of $f_1(\omega_C)$ values (*i.e.*, scaled ω_C/T_1) measured by Zajíček *et al.*[17] for $C_{9,10}$ nuclei in 1,2-dioleoyl-*sn*-glycerol-3-phosphocholine vesicles at 50 °C. Crosses – $f_1(\omega_C)$ values; short horizontal lines at crosses – estimated experimental errors in $f_1(\omega_C)$; smooth curve – $f_1(\omega_C)$ calculated by Eq. (*8*) with r = 2 and τ_i and w_i shown by vertical lines. Inset: a part of the curve with experimental data; the thin curve corresponds to a different τ_i, w_i set belonging to another local minimum in the least squares

to the overall tumbling of the vesicle, whereas that at 187.9 ps, having the amplitude of 0.2868, to highly anisotropic segmental motions. Since the NMR window allows for data in wings of both peaks only, a more detailed study of the structure of the segmental correlation time distribution can be hardly done. In the inset, large ambiguity in interpreting T_1 data is demonstrated. The thin curve shows the $f_1(\omega_C)$ function calculated with another (w_i,τ_i) set with $\tau_1 = 2.120$ ns, $w_1 = 0.02539$, and $\tau_2 = 38.39$ ps, corresponding to a different local minimum of the squares sum. The agreement is only slightly worse than that of the previous solution: a single data is reproduced with an error (only slightly) exceeding its estimated uncertainty. Were the latter solution correct, the fast segmental motions would effect complete relaxation of the bond orientations on the nanosecond scale. It turns out that T_1 (and also NOE) data cannot resolve which part of the τ amplitude missing in the NMR window is located over and which below the window's τ. It is also seen that extracting the order parameter S^2 in the model-free approach[21] may sometimes be ambiguous.

A second example shows plots of measured[13] $f_{1,T}(\omega_C)$ and $f_{2,T}(\omega_C)$ values for methine and methylene ^{13}C nuclei in poly(vinyl chloride) dissolved in dibutyl phthalate *versus* $-\log(a_T\omega_C)$ together with $f_{1,T_0}(a_T\omega_C)$ and $f_{2,T_0}(a_T\omega_C)$ functions calculated using DLM (Eq. (*13*)) parameters of ref.[13] (Fig. 4). With $f_{2,T}(\omega_C)$, calculated T_1 and measured NOE values are used to show the fit of the NOE values not disturbed by T_1 deviations. The thin curves show the $\tau w_{T_0}(\tau) \times \ln 10$ distributions, *i.e.*, the deconvoluted $f_{1,T_0}(a_T\omega_C)$ or $f_{2,T_0}(a_T\omega_C)$ functions. In insets, the plots of $1\,000/T$ *versus* $-\log a_T$ are shown to see the accuracy with which the temperature shift factors obey the Arrhenius law; $T_0 = 20$ °C. The experimental T_1 values at temperatures above 50 °C follow quite smooth curves, whereas lower-temperature data reveal much greater deviations. This may be due to a structure change between 41 and 61 °C (note that the glass transition in bulk poly(vinyl chloride) appears[22] at 83 °C). The structure change may consist in that the aggregates of poly(vinyl chloride) molecules present in the dibutyl phthalate solution[23] destroy when temperature increases. Such a destruction was observed in 1,2-dichlorobenzene[24], dibutyl oxalate[25], and diethyl oxalate[25] solutions. The associated segments are not seen in the high resolution NMR spectra; however, the aggregation is likely to influence the dynamics of the non-associated segments. The NOE values above 50 °C follow smooth curves at each particular resonance frequency; however, the curves are mutually shifted and show different maxima. This indicates a systematic error in the NOE data, the reason for which is not clear. The curves at 50.3 MHz better fit the calculated curves. The spread $\tau w(\tau)$ distributions show no traces of the

half-power singularities present in $w(\tau)$. This means that the necessity for such singularities in $w(\tau)$ is not confirmed experimentally.

The $w(\tau)$ distribution shown in Fig. 4 means that, at 20 °C, the isotropic reorientation of the C–H bond appears at as fast correlation time as 44 ns. The motional origin of such fast isotropic reorientation is not clear. The correlation time of the overall tumbling, surely effecting the isotropic reorientation, was estimated[13] to 25 μs at 30 °C. Estimating the value of 9.2 μs for 61 °C on the basis of the τ_0 dependence found in ref.[13], I tried to refine DLM parameters fixing τ_0 at 9.2 μs for 61 °C. The results were essentially the same as when fixing τ_0 at infinity. This confirms the well-known fact that the overall tumbling contributes essentially nothing to the T_1 and NOE values (they are rather insensitive to motions in the microsecond region). The latter results are shown in Fig. 5. Apparently, the calculated decrease, on the slow-time side, in the $f_{1,T_0}(a_T\omega_C)$ function (and hence in the $\tau w(\tau)$ distribution) is too slow compared to that necessary for a good fit, which the least-squares refinement compensates by increasing temperature shifts. This confirms the well-known fact that the $t^{-1/2}$ decay of the $G(t)$ function at long t is not compatible with experimental data. In the refinement, only the data above 50 °C and NOE values only at 50.3 MHz were used and different parameter sets were sought for each of methine and methylene carbons. All the τ parameters, the temperature shifts, and the α amplitude were refined simultaneously by least squares, minimizing $\Sigma(T_{1,\mathrm{exp}}/T_{1,\mathrm{calc}} - 1)^2 + \Sigma(\mathrm{NOE}_{\mathrm{calc}}/\mathrm{NOE}_{\mathrm{exp}} - 1)^2\,(T_{1,\mathrm{exp}}/T_{1,\mathrm{calc}})^2$. The last factor was introduced to linearize the problem with respect to α; it is, however, of very little effect when the T_1 fit is good. Equation (*14*) rather than Eq. (*13*) was used for DLM in order not to involve in DLM different-type terms.

To throw more light on the problem, I reconsidered the three-bond motions of a chain in the diamond lattice as a model for skeletal motions of a polymer chain. A comparison (Fig. 6) of the integral HH distribution ($\tau_0 = \infty$) with the DV result[9] ($W_4 = 0$) shows that DV cannot be approximated with HH by mere lowering[26] W_3 by 21%. W_3 should be lowered to less than one half, and DV is more diffuse than HH; the half-power singularities at the margins are still retained. The reason is that considering the discontinuities in P_a^n as continuous variations[26] is invalid even at long t since it neglects the roots of the $1/\tau(k)$ function (see ref.[9], Appendix II) other than that at $k = 0$, whereas DV has another root at $k = \pi$ even when W_4 is nonzero. This further means that DV still gives the $t^{-1/2}$ decay of $G(t)$ at long t even when four-bond motions are considered, in contrast to Eq. (*10*) of ref.[26].

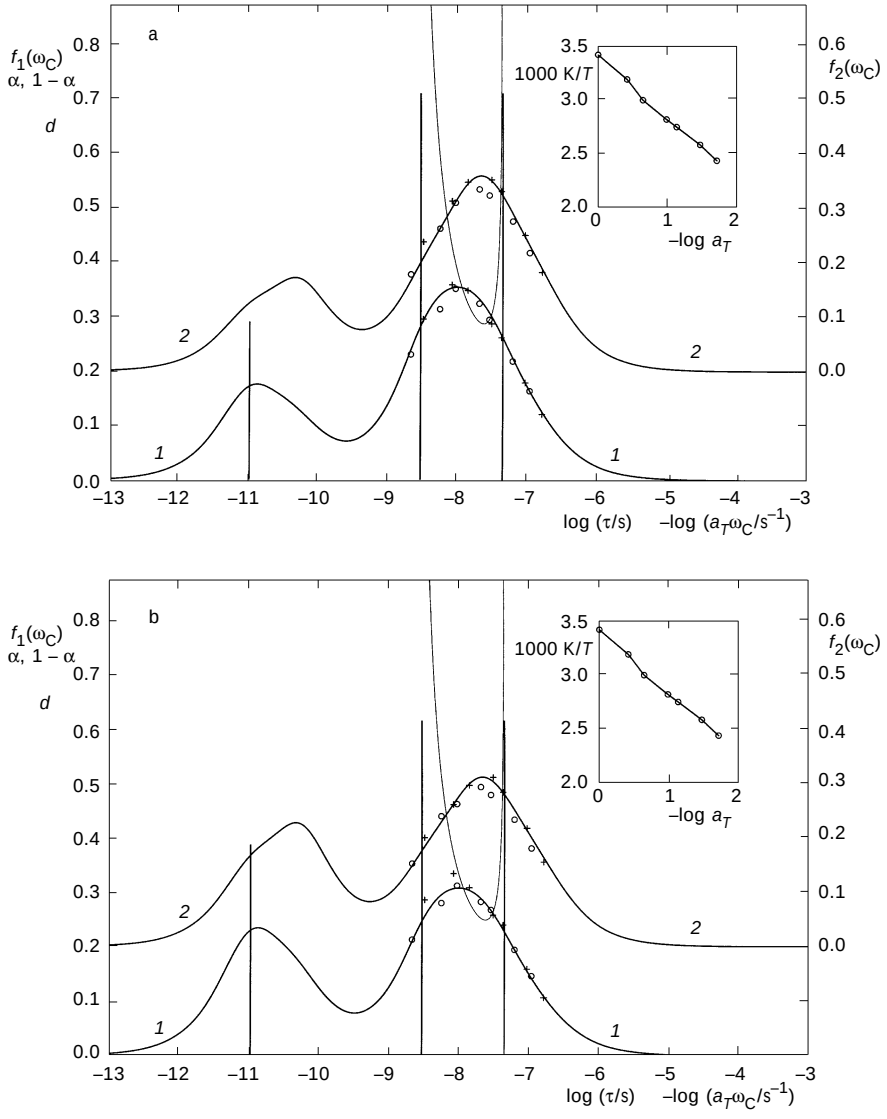

FIG. 4

Plots *versus* –log ($a_T\omega_C$) of $f_1(\omega_C)$ (*1*) and $f_2(\omega_C)$ (*2*) for methine (a) and methylene (b) nuclei in poly(vinyl chloride) dissolved in dibutyl phthalate. a_T values of ref.[13]. Experimental values[13]: the resonance frequency + 50.3 MHz, ❍ 75.4 MHz. Thick smooth curves: values calculated with parameters[13]. Vertical lines indicate the positions of τ_2, τ_1, and τ_0, their heights show the values of α and 1 – α. Thin smooth curves: the correlation time τ distributions d = ln 10 × τw(τ). Insets: plots of 1 000/T *versus* –log a_T. Reference temperature: 20 °C

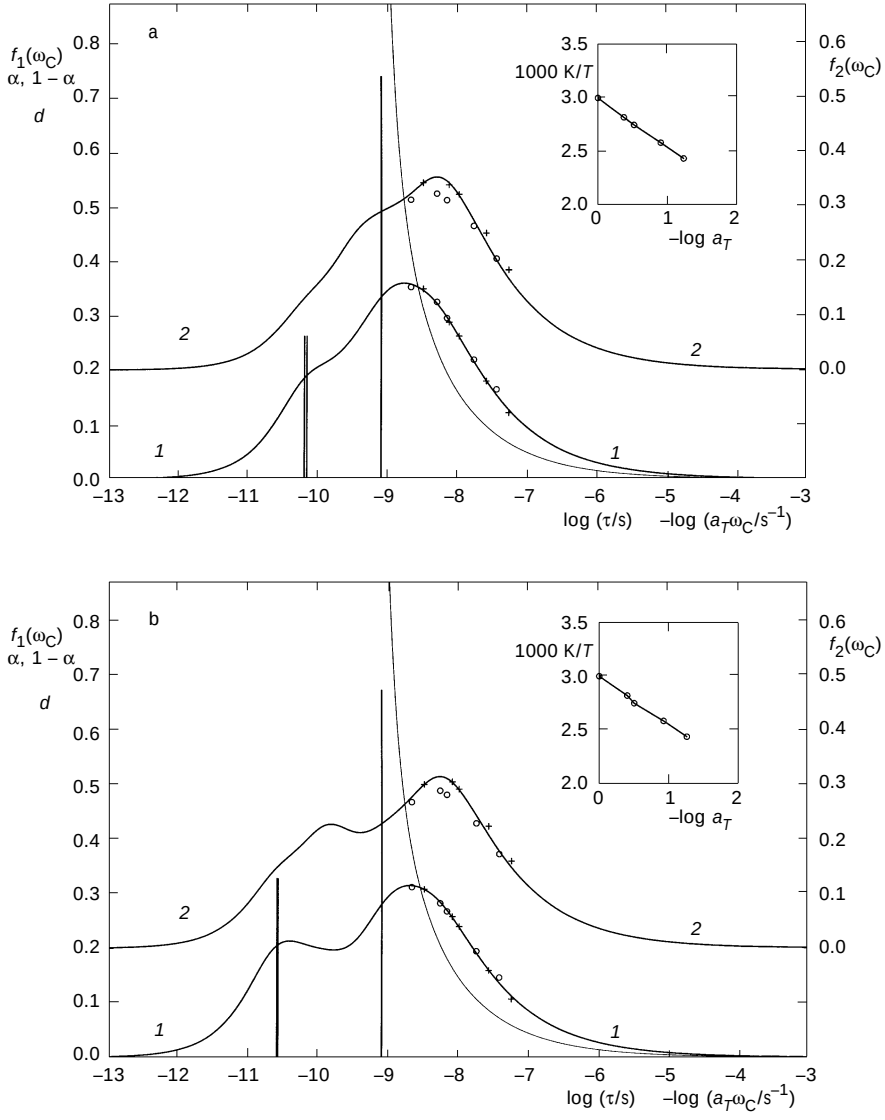

FIG. 5

The same plots as in Fig. 4 with parameters for the smooth curves and a_T factors refined using data above 50 °C, neglecting NOE values at 75.4 MHz. τ_0 fixed at infinity. Reference temperature: 61 °C. The doublet of vertical lines shows the extent of the Hall–Helfand distribution (Eq. (*11*)), the unpaired vertical line shows the value of τ_1

Describing the relaxation problem merely with P_a^n concentrations, DV estimates the P_a^n correlations and other concentrations by the maximum entropy principle, which is exact in the equilibrium state, may be, however, a crude approximation only in the course of the relaxation. To estimate the error involved, I considered the exact kinetics of the three-bond relaxation, assuming the bond direction sequence periodic with eight bonds in the period and respecting the excluded volume effect by prohibiting nonbonded chain atoms to occupy adjacent diamond lattice locations. The result compared with DV and with DV with the same periodicity condition (Fig. 7) is still more diffuse and the singularity at the fast-time margin seems smeared out. However, in view of the great width of the "slit" functions (Fig. 1), even the difference between the exact solution and HH does not seem to have an appreciable effect on the T_1 and NOE data.

In calculating the exact kinetics, I noticed that the relaxation of the non-backbone (C–H) bonds may be very different from that of the backbone (C–C) bonds considered above and I also calculated the τ distribution for the non-backbone bonds (Fig. 8). The great difference between the relaxation of the C–H and the C–C bonds is caused by the fact that only the three-bond motions over odd central bonds contribute to the relaxation of even backbone bonds and *vice versa*, whereas both "odd" and "even"

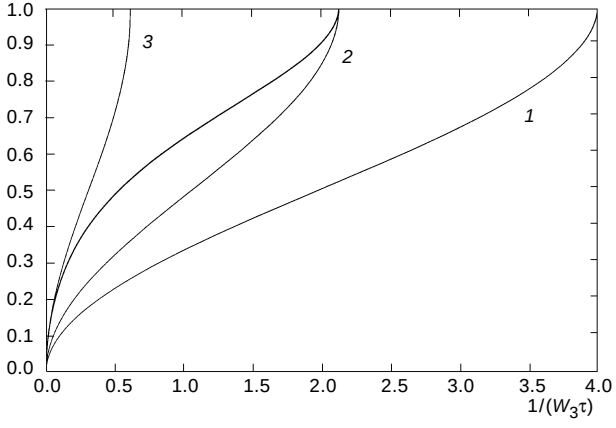

FIG. 6

Comparison of the integral Hall–Helfand distribution ($\tau_0 = \infty$) with that by Dubois–Violette ($W_4 = 0$). Thick curve: the distribution by Dubois–Violette. Thin curves: the Hall–Helfand distributions *1* W_3 unchanged, *2* W_3 scaled to give the same extent of HH as DV has, *3* W_3 scaled to give the closest touch with DV at slow τ

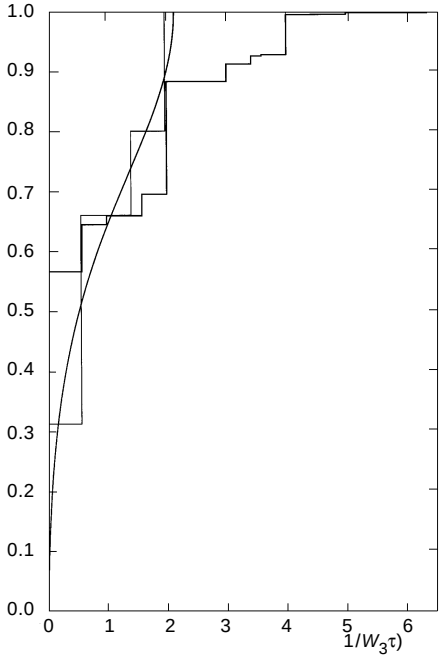

FIG. 7
Comparison of the integral Dubois–Violette distribution with the exact distribution. Smooth curve: Dubois–Violette distribution. Thin histogram: Dubois–Violette distribution with the periodic bond sequence and eight bonds in the period. Thick histogram: the exact distribution with the same periodicity condition and respecting the excluded volume effect

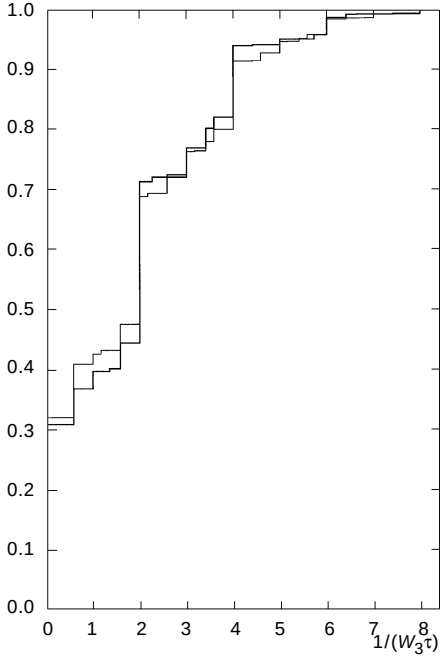

FIG. 8
Comparison of the exact integral distribution for the non-backbone C–H bonds with the periodicity condition as in Fig. 7 (the thick histogram) with that "squared" for the backbone C–C bonds (the thin histogram)

three-bond motions contribute to the relaxation of the non-backbone bonds. Were the "odd" and "even" three-bond motions independent (as in fact HH assumes),

$$G_{C-H}(t) = G^2_{C-C}(t) \qquad (20)$$

would hold. A comparison of the τ distribution for $G^2_{C-C}(t)$ with that for $G_{C-H}(t)$ under the above periodicity condition shows very little difference (Fig. 8), justifying Eq. (*20*) as a good approximation. With this, the t^{-1} decay of $G_{C-H}(t)$ at long t is expected instead of the $t^{-1/2}$ decay introduced by HH with $\tau_0 = \infty$.

The results of the refinement of the DLM parameters with HH replaced by its square and τ_0 set to infinity for the above considered poly(vinyl chloride) data are shown in Fig. 9. Note that the squared $H(\tau;\infty, 2\tau_1)$ distribution spreads from τ_1 to infinity and possesses a logarithmic singularity at $\tau = 2\tau_1$. The agreement of the experimental and calculated values is quite good and comparable with that of Fig. 4, showing that the t^{-1} decay of $G(t)$ at long t is compatible with the experimental data. A flaw of this approach is that the expression for the respective $J(\omega)$ involves the complete elliptic integral of the first kind with the complex modulus. Hence, I tried to replace the square of HH by a more simple distribution, for which a distribution uniform in $1/\tau$ (*i.e.*, the distribution (*10*) with $p = -1$) seemed useful. The result is given in Fig. 10, showing perhaps a still slightly better agreement than that in Fig. 9. This may be due to the fact that Eq. (*10*) is stronger in the long-τ queue than the square of HH; the exact three-bond τ distribution is also expected stronger in the long-τ queue than HH with infinite τ_0 (*cf.* Figs 6 and 7).

The dynamics of the dissolved atactic poly(vinyl chloride) is in fact very far from the simple three-bond model: note, *e.g.*, the differing conformer energy differences[27] in the *iso*-, *syndio*-, and *hetero*-2,4,6-trichloroheptane stereoisomers as models for poly(vinyl chloride) of the respective tacticity. Despite of this fact, no[13] or little[28] dependence of the T_1 values on the tacticity was found. The successful interpretation of the data is caused by smearing out all details of the τ distribution by wide "slit" functions (Fig. 1). Only the part of the τ distribution present in the long-τ queue seems somehow determined, due to the resolution of the "slits" uniform on the logarithmic scale. In the parameter refinement, the position of τ_2 is rather uncertain (the data are nearly insensitive to motions in the picosecond as

well as in the microsecond regions). Hence, in no way is it confirmed that the C–H librations have the same temperature τ-dependence as the segmental motions have.

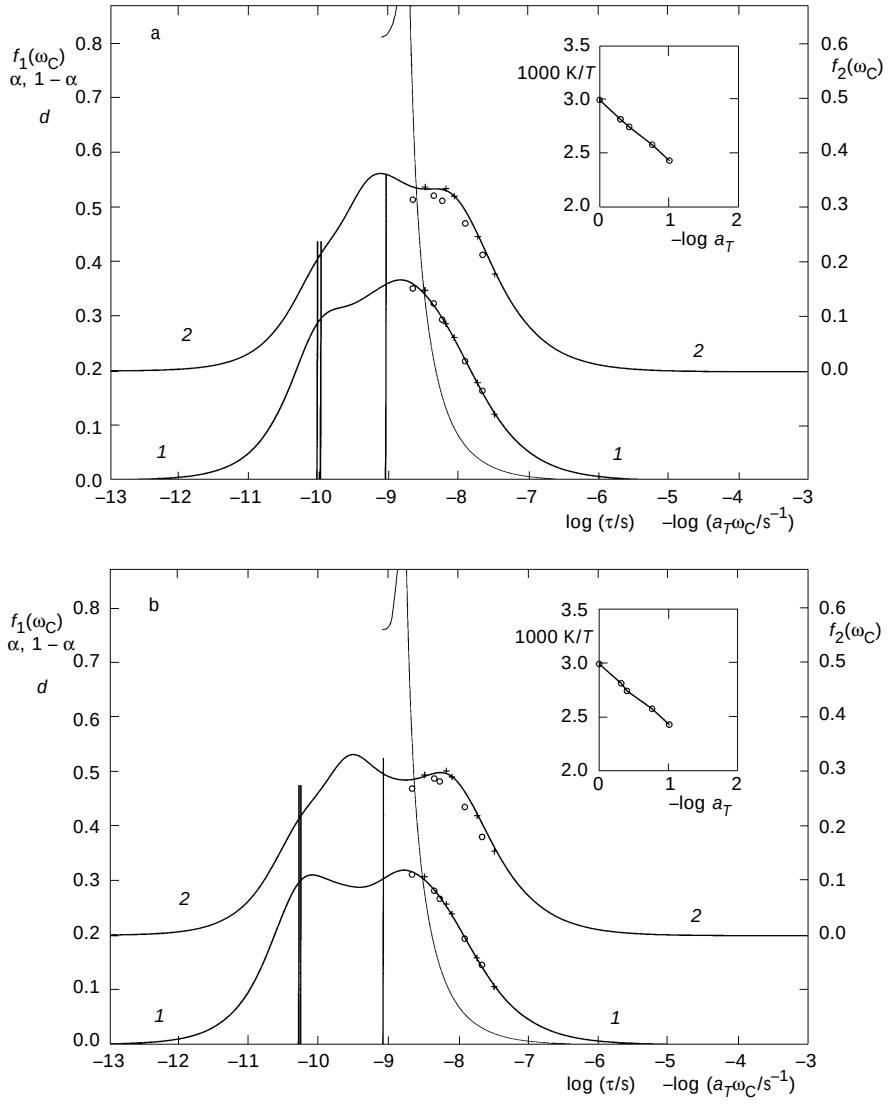

FIG. 9
The same plots as in Fig. 5 with HH in the DLM distribution replaced by its square

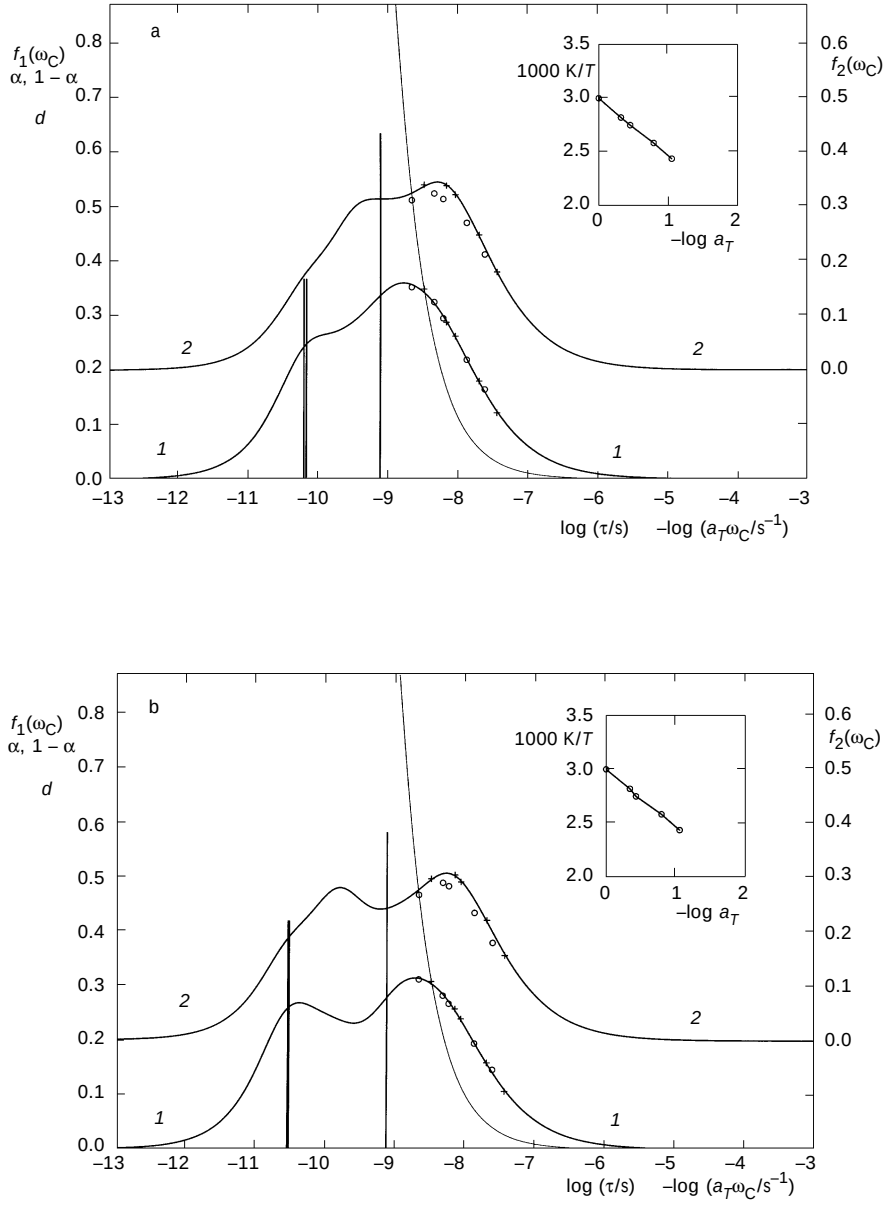

FIG. 10
The same plots as in Fig. 5 with HH in the DLM distribution replaced by a distribution uniform in $1/\tau$

Strictly speaking, the assumption that all correlation times have the same temperature dependence never holds in polymers, since activation energies of overall tumbling, methyl rotation, C–H libration, and skeletal motions are different. Practically, the correlation times of the methyl rotation and C–H libration lie in the picosecond region and that of overall tumbling lies in the microsecond region, and the actual position of a correlation time within either of these regions influences T_1 and NOE values very little (a very fast methyl rotation just increases T_1 nine times and leaves NOE unchanged when X–C–H angle is tetrahedral). Small differences in the temperature dependence of various skeletal motions (*e.g.*, between λ_0 and λ_1 in Eq. (*11*)) can be hardly detected, since the details of the τ distribution are widely smeared out by spreading with the "slit" functions shown in Fig. 1. When using just two resonance frequencies at each temperature, even large temperature dependence differences are likely to remain undetected. Hence, the ability of Eq. (*15*) to correlate T_1 and NOE data at various temperatures depends both on differences in the activation energies of various skeletal motions and on the amount and accuracy of the data. On the other hand, when log χ^2 distribution[6] showed a narrowing with increasing temperature[3], it does not mean that Eq. (*15*) cannot work with another τ distribution type. A narrowing of the τ distribution with increasing temperature follows, *e.g.*, when the uncorrelated exchange rate λ_0 in Eq. (*11*) increases with temperature faster than the correlated one λ_1.

The discrepancy between the segmental motion simulations by Geny and Monnerie[10] and by Weber and Helfand[11] should be discussed. It originates in the bad resolution of the Laplace transform inversion being one half of decade at the best[29]. From this point of view, the τ_2 correlation time, which is one half of decade to one decade slower[11] than τ_0, is more likely to represent the long-τ queue of the segmental τ distribution with the $t^{-1/2}$ decay of $G(t)$ found[10], rather than to represent the slow relaxation of the end-to-end distance as was claimed[11]. HH with infinite τ_0 fails, apparently due to the great difference between it and the actual τ distribution (*cf.* Figs 6 and 7). The absence[11] of τ_2 in $G(t)$ of the non-backbone bonds (the out-of-plane and bisector vectors) indicates that their long-τ queue is weaker in accord with what was found above, and representable by HH with a finite τ_0. The possibility to fit the above data by HH with finite τ_0 (Fig. 4) on the one hand and by the square of HH with infinite τ_0 (Fig. 9) or by distribution (*10*) (Fig. 10), both having t^{-1} decay of $G(t)$ at long t, on the other supports this interpretation. In this respect, τ_0 of HH can be seen not to have any motional origin; however, it is just a phenomenological parameter compensating the difference between the HH and actual distributions. From this

point of view, the Hall–Helfand distribution (*11*) is inadequate for a description of the relaxation of the non-backbone chain bonds by segmental motions: it is inappropriate to use a distribution with singularities having neither theoretical nor experimental support, when a simpler distribution with one parameter less (Eq. (*10*)) fits the data.

Figure 8 shows that the jump at short-τ margin is probably smoothed. If experimental data show a necessity for such a smoothing, distribution (*10*) should be replaced by the generalized exponential (GEX) distribution[30,31]

$$w(\tau) = |s| \tau^{p-1} \tau_0^{-p} \exp\left(-(\tau / \tau_0)^s\right) / \Gamma(p/s) \qquad (21)$$

with $p = -1$ and a finite negative s ($s = -\infty$ gives the distribution (*10*)). If, in Eq. (*10*) or (*21*), a refinement of p to a value different from –1 were tried, p would be expected to compensate the difference between the used and actual distributions, rather than to give the actual decay of the τ queue, due to the limited extent to long τ of the NMR window.

Although, in the short-time region, the exact solution with the eight-periodicity condition (Figs 7 and 8) seems fine enough due to the wide spreading caused by the "slits", it cannot estimate the form of the long-τ queue reliably. Even extending the period up to sixteen chain bonds (this calculation can be hardly performed by recently accessible means) is unlikely to give substantially more information. Hence, I give a speculative consideration of the matter. The purely diffusive relaxation of the bond orientation gives the $t^{-1/2}$ decay of $G(t)$ since the excess of the orientation of the bond being relaxed (*i.e.*, $P_a^0 = 1$ instead of the equilibrium value of 1/4) is not lost but only dissipated, and hindering by the backstep effect may only slow down the decay. (The exponential decay of the Jones–Stockmayer model[32] (JS) does not contradict this since, in JS, a half of the relaxation of the terminal bonds of the interacting segment proceeds non-diffusively.) Hence, the three-bond model should yield the $t^{-1/2}$ decay or slower for the backbone and t^{-1} or slower for the non-backbone bonds. The four-bond motions provide non-diffusive relaxation of the bond orientation. With DV approximation[9], the decay is still $t^{-1/2}$ (see above). Under the eight-periodicity condition, including four-bond motions, up to 2/3 of the excess is lost in some conformations. With a periodicity long enough, complete loss is possible, allowing speeding up the decay. However, the suitable conformations are very rare, so that the non-diffusive relaxation can be hardly

expected faster than the overall tumbling. Hence, the exponential decay of $G(t)$ should be expected on the time scale of overall tumbling only.

CONCLUSIONS

The plots of ω/T_1 and NOE × ω/T_1 values *versus* –log ω were found to represent the distribution of the orientational correlation time τ spread with rather wide "slit" functions and as such very useful in correlating T_1 and NOE data at various resonance frequencies ω. For correlating data at various temperatures, the plots *versus* –log (ωa_T) should be used, with temperature shift factors a_T following the Arrhenius or Williams–Landel–Ferry equation, or with the factors obtained by a parameter refinement. On the basis of the plots and of a consideration of the segmental motion dynamics, the Hall–Helfand distribution of the correlation time τ was found inadequate for the description of the orientational relaxation by the segmental motions of the non-backbone (C–H) bonds in a polymer chain. An alternative distribution was suggested. The orientational relaxation of the non-backbone chain bonds was found considerably different from that of the backbone bonds.

The support by the Grant Agency of the Czech Republic (grant No. 203/95/1319) is gratefully acknowledged.

REFERENCES

1. Abragam A.: *The Principles of Nuclear Magnetism*, Chap. VIII. Clarendon Press, Oxford 1961.
2. Allerhand A., Doddrell D., Komoroski R.: *J. Chem. Phys.* **1971**, *55*, 189.
3. Gao Z., Zhong X.-F., Eisenberg A.: *Macromolecules* **1994**, *27*, 794.
4. Kuhlmann K. F., Grant D. M., Harris R. K.: *J. Chem. Phys.* **1970**, *52*, 3439.
5. Doddrell D., Glushko V., Allerhand A.: *J. Chem. Phys.* **1972**, *56*, 3683.
6. Schaefer J.: *Macromolecules* **1973**, *6*, 882.
7. Monnerie L., Geny F.: *J. Chim. Phys.* **1969**, *66*, 1691.
8. Hall C. K., Helfand E.: *J. Chem. Phys.* **1982**, *77*, 3275.
9. Dubois–Violette É., Geny F., Monnerie L., Parodi O.: *J. Chim. Phys.* **1969**, *66*, 1865.
10. Geny F., Monnerie L.: *J. Chim. Phys.* **1969**, *66*, 1872.
11. Weber T. A., Helfand E.: *J. Phys. Chem.* **1982**, *87*, 2881.
12. Dejean de la Batie R., Lauprêtre F., Monnerie L.: *Macromolecules* **1988**, *21*, 2045.
13. Radiotis T., Brown G. R., Dais P.: *Macromolecules* **1993**, *26*, 1445.
14. Dais P., Nedea M. E., Morin F. G., Marchessault R. H.: *Macromolecules* **1989**, *22*, 4208.
15. Guillermo A., Dupeyre R., Cohen-Addad J. P.: *Macromolecules* **1990**, *23*, 1291.
16. Gisser D. J., Glowinkowski S., Ediger M. D.: *Macromolecules* **1991**, *24*, 4270.

17. Zajíček J., Ellena J. F., Williams G. D., Khadim M. A., Brown M. F.: *Collect. Czech. Chem. Commun.* **1995**, *60*, 719.
18. Brown M. F.: *J. Chem. Phys.* **1984**, *80*, 2832.
19. Ferry J. D.: *Viscoelastic Properties of Polymers*, Chap. 11. Wiley, New York–Chichester–Brisbane–Toronto 1980.
20. Williams M. L., Landel R. F., Ferry J. D.: *J. Am. Chem. Soc.* **1955**, *77*, 3701.
21. Lipari G., Szabo A.: *J. Am. Chem. Soc.* **1982**, *104*, 4559.
22. van Krevelen D. W., Hoftyzer P. J.: *Properties of Polymers: Correlations with Chemical Structure*, p. 114. Elsevier Publishing Company, Amsterdam–London–New York 1972.
23. Spěváček J., Suchopárek M.: *Macromolecules* **1997**, *30*, 2178.
24. Spěváček J., Schneider B.: *Makromol. Chem.* **1975**, *176*, 3409.
25. Spěváček J., Suchopárek M., Mijangos C., López D.: *Macromol. Chem. Phys.* **1998**, *199*, 1233.
26. Valeur B., Jarry J.-P., Geny F., Monnerie L.: *J. Polym. Sci., Polym. Phys. Ed.* **1975**, *13*, 667.
27. Doskočilová D., Štokr J., Schneider B., Pivcová H., Kolínský M., Petránek J., Lím D.: *J. Polym. Sci., Part C: Polym. Symp.* **1967**, *16*, 215.
28. Inoue Y., Nishioka A., Chujo R.: *J. Polym. Sci., Polym. Phys. Ed.* **1973**, *11*, 2237.
29. Jakeš J., Štěpánek P.: *Czech. J. Phys. B* **1990**, *40*, 972.
30. Kubín M.: *Collect. Czech. Chem. Commun.* **1967**, *32*, 1505.
31. Jakeš J., Saudek V.: *Makromol. Chem.* **1986**, *187*, 2223.
32. Jones A. A., Stockmayer W. H.: *J. Polym. Sci., Polym. Phys. Ed.* **1977**, *15*, 847.